Remote Sensing of Environment 123 (2012) 593–599

Contents lists available at SciVerse ScienceDirect

Remote Sensing of Environment

journal homepage: www.elsevier.com/locate/rse

Observation of oceanic origin of Sahel precipitation from space

W. Timothy Liu [a,*], Xiaosu Xie [a], Kristina B. Katsaros [b]

[a] Jet Propulsion Laboratory, California Institute of Technology, Pasadena, CA 91109, United States
[b] Rosenstiel School of Marine and Atmospheric Sciences, Miami, FL 33249, United States

ARTICLE INFO

Article history:
Received 15 July 2011
Received in revised form 9 April 2012
Accepted 16 April 2012
Available online xxxx

Keywords:
West African Monsoon
Sahel rainfall
Remote sensing
Ocean–atmosphere–land interaction

ABSTRACT

The West African Monsoon region is of great concern due to the negative ecological, economical, and societal impacts of the persistent drought. Our results support the established postulation that the onset of summer rain in the southern region is associated with the migration of the inter-tropical convergence zone and in phase with the meridional moisture transport from the Gulf of Guinea. We present recent satellite measurements that illustrate the phase shift of the precipitation in the northern region, the Sahel, with respect to the region to the south. These satellite data and associated analysis techniques let us combine the effect of the onshore flow at the surface and offshore transport aloft to demonstrate with sufficient clarity that the depth-integrated moisture advection across the west coast, from the open Atlantic Ocean into the Sahel region, is in-phase with the annual and inter-annual variations of Sahel rainfall, but out-of-phase with rainfall in the southern region around the Gulf of Guinea. The peak Sahel rainfall is associated with the short-lived net moisture influx from the Atlantic, which may interact with local instability related to the African Easterly Waves. The data show two precipitation regimes in Western Africa Monsoon region associated with moisture input from two different regions of the ocean.

1. Introduction

The world became aware of the socioeconomic vulnerability of the agricultural societies in the Sahel region of West Africa to the vagaries of summer rainfall during the disastrous 1970s drought (Mortimore & Adams, 1999), which extended into the 1980s. The African Monsoon Multidisciplinary Analysis, an international research project and field campaign (Redelsperger et al., 2006), has since attempted to get a better understanding of the West African Monsoon (WAM) system. We will refer to the region between the Sahara and the Gulf of Guinea as the WAM area in this study. Surface data are still limited and do not provide the large spatial view provided by observations from space. Satellite infrared sensors observe cloud cover and have been used to define weather systems and to support measurements by surface rain gauges (e.g. Bell & Lamb, 2006; Rowell & Milford, 1993). Here we bring in satellite microwave sensors and new techniques to reveal the oceanic origin of the cause for the phase shift of monsoon onset (also referred to as 'precipitation jump') in the region. Space-based sensors are not limited by geopolitical boundaries and can potentially provide continuous monitoring of the WAM area where the Sahel is located.

Our study focuses on a rather abrupt transition of rainfall in the WAM area, which has been well observed and discussed (e.g., Gu & Adler, 2004; Hagos & Cook, 2007; Le Barbe et al., 2002; Lebel et al., 2003; Redelsperger et al., 2002; Sultan & Janicot, 2000). Monthly precipitation, from the Tropical Rainfall Measuring Mission, TRMM, shown in Fig. 1 for an eight-year period (July 1999 to June 2007), illustrates the transition (see Section 2 for description of the data). Rainfall peaks in June south of 8°N, but in August to the north. In the south, there is a second peak in September after a relatively dry period. The figure also illustrates the short rain season in the north and the large inter-annual variability there. We will refer to the area between 8 and 16°N as the Sahel. The prevailing attribution of the variation of rainfall in the south has been the seasonal migration of the inter-tropical convergence zone (ITCZ) and corresponding meridional circulation that brings moisture from the Gulf of Guinea over land (Sultan & Janicot, 2000). Our results support this postulation. Rainfall in the Sahel has also been attributed to ITCZ migration in summer through data analysis (e.g. Lebel et al., 2003) and a regional climate model (Hagos & Cook, 2007). The additional effect of the meridional shift of the easterly jet was also suggested (Fontaine et al., 1995; Redelsperger et al., 2002). The two-month phase shift between Sahel and the southern region of WAM, however, has not been explained through observations and dynamical models with finality.

Many studies have postulated and illustrated that the Sahel rainfall is controlled by synoptic scale convection associated with easterly waves that propagate westward with the easterly jet (Bell & Lamb, 2006; Fink & Reiner, 2003; Matthews, 2004; Nicholson & Grist, 2003; Rowell & Milford, 1993; Sultan & Janicot, 2003). Although Lebel et al. (2003) recognize an oceanic rainfall regime caused by migration of the ITCZ from the south, they claim that a continental regime, consisting

* Corresponding author. Tel.: +1 818 354 2394.
E-mail address: W.T.Liu@jpl.nasa.gov (W.T. Liu).

0034-4257/$ – see front matter
doi:10.1016/j.rse.2012.04.007

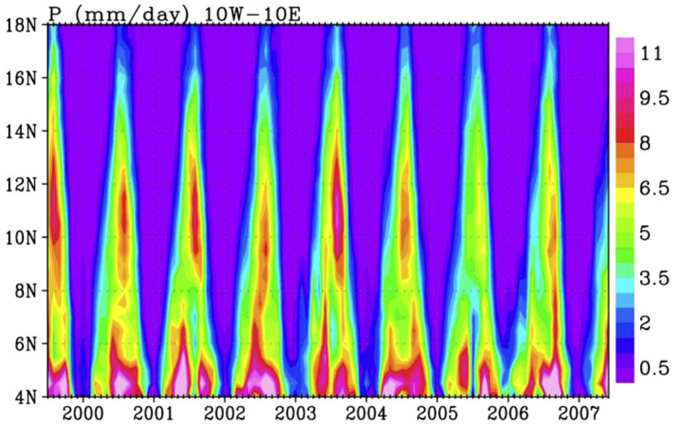

Fig. 1. Precipitation jump in the WAM area, July 1999–June 2007. Latitude-time variation of monthly-mean precipitation (in mm/day) from TRMM, averaged between 10°W and 10°E over land. The latitude runs from the Gulf of Guinea in the south to the Sahara in the north.

of a small number of large convective systems imbedded in the easterly circulation is responsible for 75–90% of the yearly rainfall. These convective systems occur in June but not in August. There is no other clear evidence of phase coherence between rainfall and the strength of easterly waves in annual and inter-annual variations in the Sahel. The easterly jet is blowing air from land out to the Atlantic instead of bringing moisture from the ocean to feed the summer rainfall. Although rain is a synoptic event associated with local instability, which may be caused by the easterly waves, the aggregate of these events should agree with the seasonal variation of rainfall and oceanic influence, which is the essence of a monsoonal circulation.

The variability of Sahel rainfall in the inter-annual and longer time scales has been put in global context, mainly through its relation with the global distribution of sea surface temperature (e.g., Chang et al., 2008; Folland et al., 1986; Giannini et al., 2003; Janicot et al., 2001; Lamb & Peppler, 1992; Okumura & Xie, 2004; Rowell, 2001; Vizy & Cook, 2002; Zheng et al., 1999), but one would think that the long-term teleconnections should be reflected in the local seasonal reversal of transport between ocean and land, which is the basic definition of a monsoon.

The moisture transport (integrated over the depth of the atmosphere) across the coastline is the most relevant parameter to represent the oceanic influence on continental rainfall. More than two decades ago, Cadet and Nnoli (1987), using integrated moisture transport computed from operational data of the European Center for Medium Range Weather Forecasts (ECMWF), recognized the influence of northward advection of moisture from the Gulf of Guinea on the rainfall in the WAM region. They suggested that northward advection is drawn in by the easterly waves. Moisture advection computed from atmospheric reanalysis data of the National Center for Environmental Prediction (NCEP) was used by Fontaine et al. (2003) to study the water balance of the WAM region. These studies did not reveal with certainty the underlying reason for the precipitation jump, but we hope to shed some light on it here. With unprecedented resolutions of the integrated moisture transport calculated with the help of satellite data, particularly in the west-coast region of Africa, where atmospheric soundings are sparse, this study purports to show the essential role of column integrated moisture transport across the southwest coastline of the WAM-region bringing moisture from the open Atlantic Ocean to support peak Sahel summer rainfall.

2. Methods and data

A combination of spacebased sensors is used to estimate the depth-integrated moisture advection,

$$\Theta = \frac{1}{g}\int_0^{p_s} q\mathbf{u}dp \tag{1}$$

where g is the acceleration due to gravity, p is the pressure, p_s is the pressure at the surface, q and **u** are the specific humidity and wind vector at a certain level. The vertical profiles of wind vector and humidity are measured only at rawinsonde locations that are very sparse over ocean. There are more data on ocean–land transport at the surface, but they are quite different from Θ along the Atlantic coast of the WAM region, because the transport aloft is often in opposite direction to the surface flow. A statistical model to estimate Θ over the ocean from three space measurements, surface wind vector from scatterometer, cloud drift wind, and integrated water vapor (W) has been developed (Liu & Tang, 2005; Xie et al., 2008). W is defined as

$$W = \frac{1}{g}\int_0^{p_s} qdp. \tag{2}$$

In this method, Θ may be viewed as a column of water vapor, W, moved at an equivalent velocity (u_e), $\mathbf{\Theta} = \mathbf{u}_e\mathbf{W}$. The equivalent velocity can be thought of as the ratio of Θ to W (Eqs. 1 and 2), equivalent to the depth averaged wind vector weighted by humidity. It is related statistically to wind vectors at two levels. In deriving Θ, all the data, including surface equivalent neutral wind from QuikSCAT (described below), cloud drift wind from the National Oceanic and Atmospheric Administration (NOAA), and integrated water vapor from the Special Sensor Microwave/Imager (SSM/I), are averaged to daily 0.5° resolution before inputting into the statistical model (Xie et al., 2008).

QuikSCAT is a Ku-band radar launched in 1999 that has provided surface wind vectors, covering 90% of global ocean daily (see review by Liu, 2002). NOAA has produced cloud drift winds by automatically tracking cloud motions at various levels (Hayden et al., 1994). The winds between 800 mb and 900 mb are averaged and used in this study. SSM/I is an operational multi-frequency microwave radiometer and a series of the instruments has produced integrated water vapor operationally since 1987 (Wentz, 1997).

For training the statistical model, using Support Vector Regression, Xie et al. (2008) used 10,000 randomly selected values of Θ, computed from wind and humidity profiles of NCEP reanalysis, to complement Θ derived from rawinsondes. In addition to the 10,000 data randomly selected from rawindsondes between 40°N and 40°S, all rawinsondes data poleward of 40° (over 6000) were used. Realizing that there are differences between the reanalysis of NCEP and ECMWF, a new statistical model was built, replacing the training data from NCEP with the average of NCEP and ECMWF data at the same spatial and temporal grids. The Θ data set is accessible through http://climatesciences.jpl.nasa.gov/ClimateDataRecords/EvapoationData and has been extensively tested against those derived from rawinsondes, with similar results as found by Xie et al. (2008). Hilburn (2010) found very good agreement between this data set and data computed from Modern Era Retrospective-analysis for Research and Applications (MERRA) over the global ocean. MERRA is a NASA atmospheric reanalysis using a major new version of the Goddard Earth System Data Assimilation System (Rienecker et al., 2011).

The closest rawinsonde stations in the Atlantic are to the north of the Sahel and the Θ derived from rawindsondes agrees well with modeled-derived Θ from daily to monthly variations. For example, at Cape Verdes islands (16.73°N, 337.05°E), the zonal component of Θ strongly dominates over the meridional component, and the 306 pairs of daily data in 2002 give a root-mean-square (RMS) difference of 67.8 in a range of about 600 kg/m/s and a correlation coefficient of 0.92. For Santa Cruz in the Canary Islands (28.45°N, 16.2°W), the 278 pairs of zonal components give a RMS difference of 42.42 in a range of 500 kg/m/s and a correlation coefficient of 0.89.

Spacebased observations have been used to estimate rainfall in the past two to three decades, and TRMM has provided important calibration since 1998. TRMM is composed of a radar and a microwave imager flying in a low-inclination orbit to provide high frequency rain measurements between 38° latitude north and south of the equator. The TRMM data product 3B42 (Huffman et al., 2007), a merged infrared and microwave spacebased data set, with 3-hourly, 0.25°×0.25° resolutions and extended coverage to 50°, was averaged into monthly resolution and used in this study. Although comparing satellite products and gauge measurements is difficult due to difference in resolution, the examples shown in Fig. 2 show that the TRMM data set used in this study picks up the timing and magnitude of the summer rainfall measured at surface weather stations (made available to us courtesy of A. Fink).

Sea surface temperature (SST) is measured by the Advanced Microwave Scanning Radiometer (AMSR), and our data set is acquired from Remote Sensing Systems. All data set used in this study span an eight year period from July 1999 (when QuikSCAT data started) to June 2007, except for AMSR data, which are available starting June 2002.

3. Results

The components of Θ normal to two simplified coastlines (integrated over the length of the coastlines) were computed; one runs northwest to southeast along the coast facing the open Atlantic Ocean (labeled as A in Fig. 3a) and the other runs east to west along the Gulf of Guinea (labeled as B in Fig. 3b). Positive is for onshore (in direction of the arrows) and negative for offshore advection normal to either line A or B. The 95% confidence level for the correlation coefficients between Θ and TRMM rainfall in Fig. 3, for 96 months of data records is $1.98/\sqrt{N-2}=0.2$, where N is the number of data (Panofsky & Brier, 1968), and the value is marked by a white contour in the figure. Fig. 3a shows that the Θ coming onshore across A from the open Atlantic has significantly high contemporary correlation with rainfall in the Sahel region, but not with rainfall in the southern region near the Gulf of Guinea. In contrast, the northward Θ from the Gulf of Guinea has strong correlation with rain just near the coast of the Gulf of Guinea but much weaker correlation with the rain further north in the Sahel (Fig. 3b). The correlation maps show two precipitation regimes separated at about the latitude 8°N in a line between the Atlantic coast and 20°E. The first regime, covering the Sahel (between 8°N and 16°N), is dominated by Θ from the open Atlantic Ocean to the west, and the other one between 8°N and the coast of the Gulf of Guinea is dominated by Θ from the south.

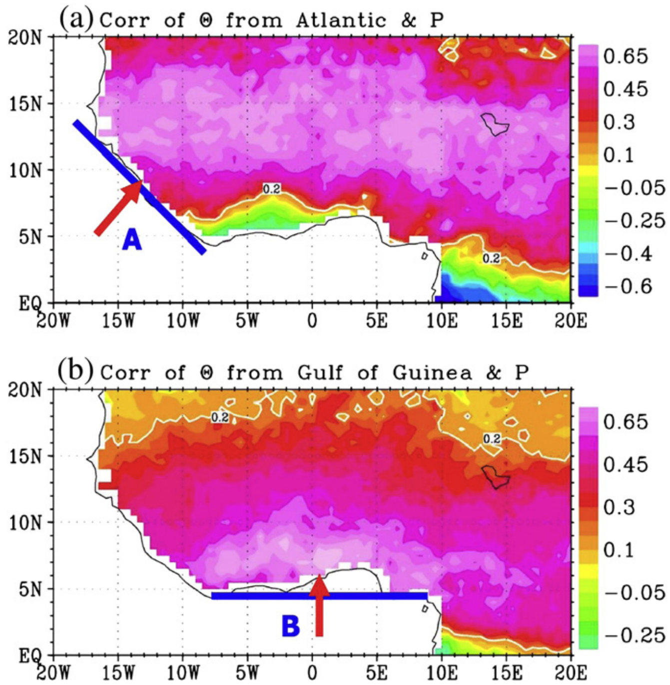

Fig. 3. Distribution of the contemporary temporal correlation coefficient between monthly mean precipitation over the WAM region measured by TRMM and the integral of on-shore components of Θ normal to the simplified coastlines A from the open Atlantic (a) and B from the Gulf of Guinea (b). The white lines represent 95% confidence level.

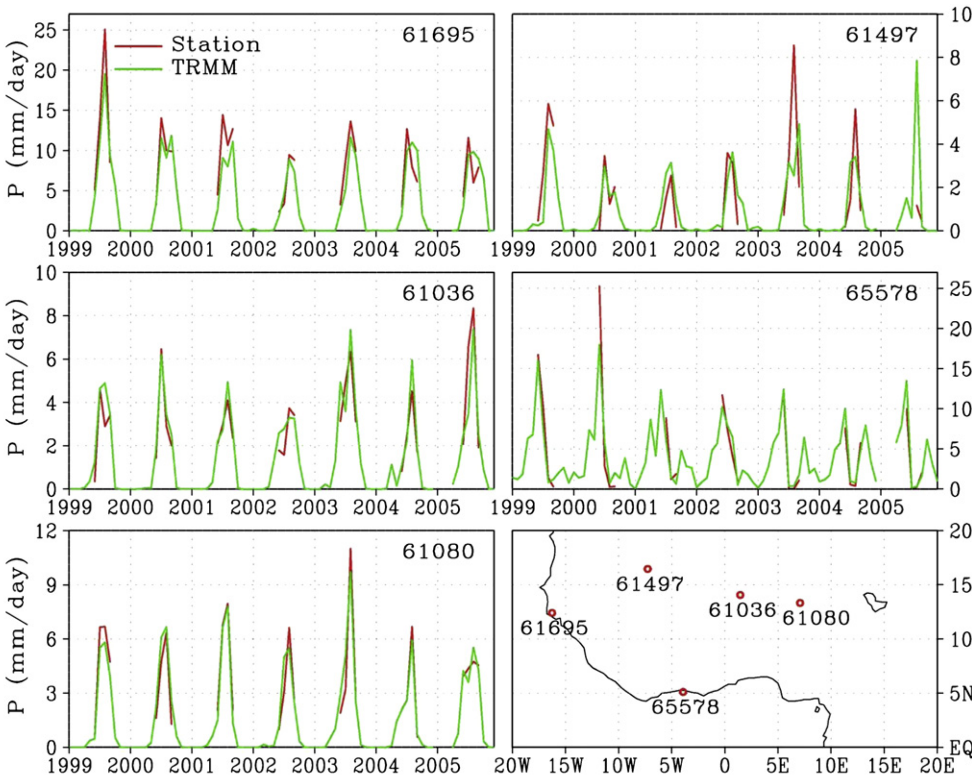

Fig. 2. Comparison of TRMM precipitation with measurements at 5 selected stations in the WAM region provided courtesy of A.H. Fink. The locations of the stations are shown in the lower-right panel.

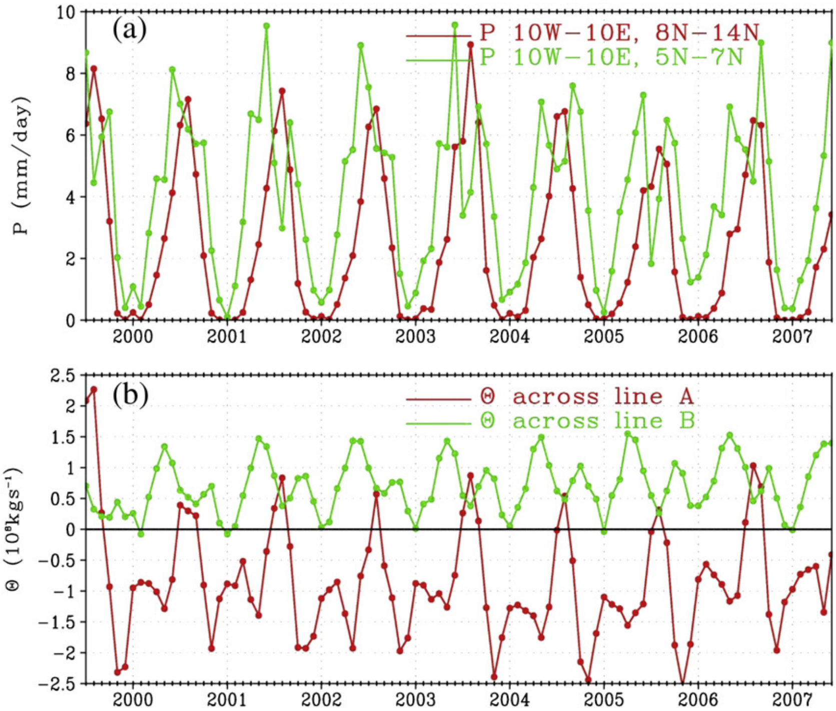

Fig. 4. Time series of TRMM precipitation integrated over the northern and southern parts of the WAM area (a), and time series of the Θ component normal to the coastlines A and B, and integrated over the length of the coastlines (b). (For interpretation of the references to color in this figure legend, the reader is referred to the web version of this article.)

The time series of average rainfall in the center of the continental areas (boundaries are a bit arbitrary) are shown in Fig. 4a. They show that the rainfall in the southern region (green) has two peaks, and the rainfall in the northern region (red) has a single peak that lags the first peak (onset) of the southern region by two months, demonstrating the 'precipitation jump'. The time series of Θ component used in Fig. 3 are shown in Fig. 4b. Fig. 4b shows that Θ from the Gulf of Guinea across line B (Fig. 3b) has two peaks, similar to precipitation in the southern region. While the first peak of Θ coincides with the first peak of rain, the second Θ peak lags behind the second rain peak. Across line A from the open Atlantic, Θ comes onshore only in the summer months centered in August. The 'precipitation jump' may be the result of the phase difference between Θ from the Gulf of Guinea and that from the open Atlantic to the west. The rain onsets in the northern and southern regions are coincident with the first peak values of onshore Θ across A and B respectively.

This phase shift of the transport was not realized by those who examined the more accessible ocean surface wind vectors. Upper level wind and humidity measurements were sparse at this coastline. Surface transport has quite a different annual cycle than Θ across coastline A as shown in Fig. 5. While surface winds (from QuikSCAT) are onshore almost year round, Θ goes offshore except around August (in the monthly average). This is further demonstrated by the maps of surface wind and Θ vectors near coastline A in Fig. 6, for the year 2003 as an example. In June, during the monsoon onset in the southern region, surface winds blow onshore, but Θ comes offshore and along shore and brings no net moisture into the Sahel region. Two months later, in August, Θ lines up with the surface wind (south of 10°N) and brings moisture from the Atlantic to the Sahel region. Over the WAM area, the seasonal variation of Θ is found to be quite different from the surface transport because surface advection from the Atlantic (onshore) is offset by upper level advection by the easterly waves in the opposite direction (offshore). Although the opposite flow directions were known in the past, the net effect on the total water flow has not been sufficiently discussed without the benefit of high resolution spacebased observations.

The cause of the August rainfall peak is explored with SST in Fig. 7. The SST (from AMSR-E) in the Atlantic west of coastline A, at 7°N, 17°W, shows a strong negative correlation with on-shore Θ from the Atlantic Ocean (Fig. 7). Water temperature is lowest in August, corresponding to the positive Θ from the Atlantic. Cooler water and warmer land set up the pressure gradient for onshore transport, supporting the classical description of a monsoon. The onshore Θ and land–ocean pressure gradient in August is consistent with the low level westerly jet

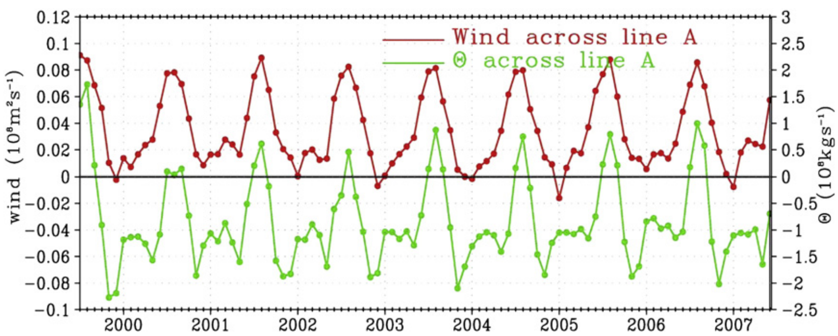

Fig. 5. Time series of the normal components of surface wind and Θ integrated over the length of coastline A in Fig. 3a.

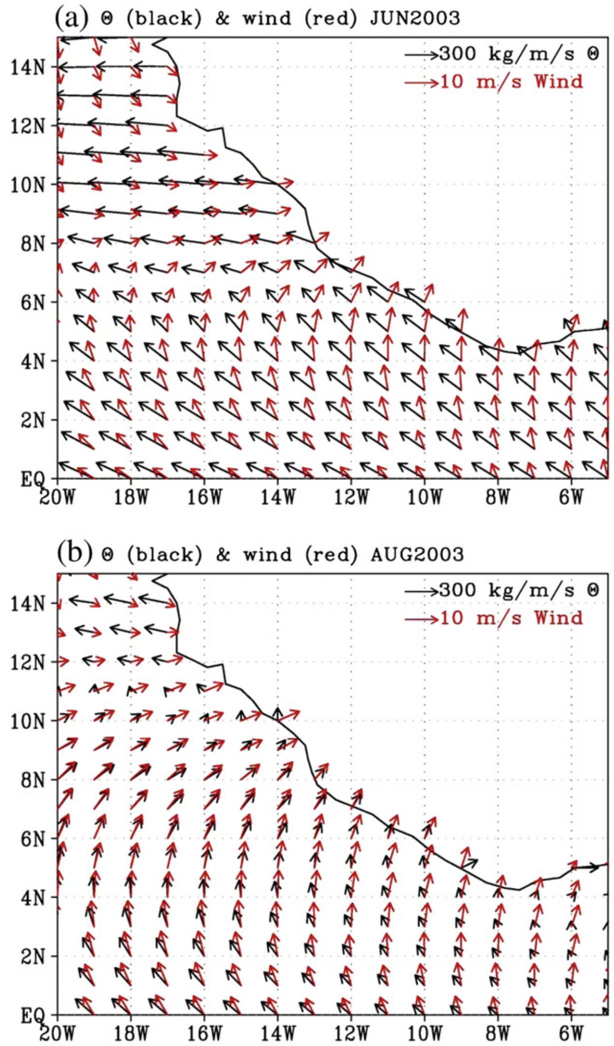

Fig. 6. Surface wind vector (red) and Θ vector (black) for June (a) and August (b) of 2003. (For interpretation of the references to color in this figure legend, the reader is referred to the web version of this article.)

identified by Grodsky et al. (2003) using scatterometer data. Pu and Cook (2010) studied the dynamics of this jet as distinguished from monsoon flow using reanalysis output.

The easterly jet is the result of vertical wind shear in the troposphere (the so called thermal wind) developed in response to the meridional density (temperature and moisture) gradients over the West African landmass between the Gulf of Guinea and the Sahara, with a maximum at the 600–700 mb level. Present spacebased sensors do not measure wind vectors over land. Although numerical models suffer from large systematic errors in this region (Davey et al., 2002; Redelsperger et al., 2006; WCRP, 2011), NCEP products show that winds aloft at the Sahel are easterly most of the year, with broad peaks during summer, but weaken in August, when the Sahel rainfall peaks (not shown). The August break in the strong easterlies is more obvious in the south than in the north. The implication is that the onshore moisture transport from the Atlantic is confined to the surface with offshore transport (easterly) aloft most of the time. During August, the onshore transport (westerly) extends further up in the troposphere, resulting in a net import of moisture with the associated instability for the heaviest rainfall in the Sahel.

Even though the time series of available satellite data is not very long, we attempt to compute the inter-annual anomalies by removing the eight-year mean annual cycle from our monthly data. Although the correlation coefficients of the anomalies between rain and moisture flux across simplified coastlines A and B are low, the separation of the two rainfall regimes associated with moisture flux across the simplified coastlines can still be discerned from the statistically significant (>0.2) region, as shown in Fig. 8a and b. These statistically significant regions are smaller than those shown in Fig. 3, and smaller regions are selected for the time series comparison in Fig. 9a and b. Over the Sahel, there is agreement, except for the year 2005. The associations between rain and Θ appear to be quite similar to those for the annual cycle. NCEP data (not shown) indicate stronger summer easterlies in the dry years than the wet years. This is consistent with the analysis of Fontaine et al. (2003). The moisture advection from the Atlantic that influences the seasonal variation of Sahel rainfall also influences the magnitudes of the inter-annual anomalies.

4. Conclusion/discussion

Our finding is at variance with prevailing postulations that Sahel rainfall variation is controlled a) by the meridional moisture transport from the Gulf of Guinea in the south, which, as we show, is out-of-phase with the annual cycle of Sahel rainfall, or b) by the synoptic scale instability in the easterly jet, which we suggest cannot be the full explanation since the jet blows over the eastern mountain range and dry soil of the continent out to the Atlantic Ocean rather than bringing moisture in. Cadet and Nnoli (1987) first indicated that moisture transport aloft by the easterlies out of the continent should not affect Sahel rainfall.

In relating the phase shift in the monsoon across a latitude in the WAM region to the phase difference between the integrated moisture transport across two sections of the coastline, we fall back to the general concept of the water cycle and the basic definition of a monsoon. Water is continuously removed from the ocean into the atmosphere as excess evaporation over precipitation, redistributed through atmospheric circulation, deposited as excess precipitation over evaporation on land, and returned to the ocean as river discharge. Over extensive continental areas, the precipitation could not be sustained solely by land evaporation and needs moisture transported on shore from the

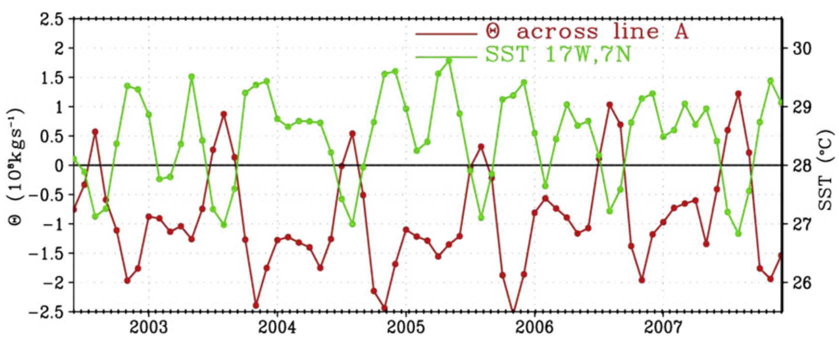

Fig. 7. Time series of the Θ component normal to the coastline A (integrated over the length of the coastline) and corresponding SST at 17°W and 7°N, just to the west of this coastline.

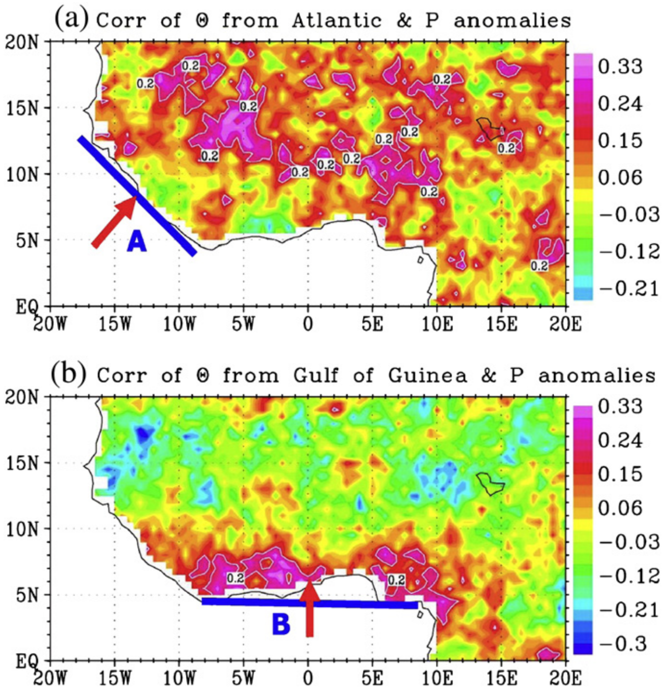

Fig. 8. Same as Fig. 3, except for the interannual anomalies instead of monthly mean.

ocean. A monsoon is the seasonal reversal of wind direction and moisture transport between ocean and land that has rain as a consequence.

It is evident that the summer rain onset in the southern region near the Gulf of Guinea is associated with the northward transport of moisture from the Gulf of Guinea as postulated in many past studies. In addition, we have shown that the annual and inter-annual variabilities of the rainfall in the Sahel region to the north are dependent on the moisture transport, not so much from the Gulf in the south, but from the open Atlantic Ocean to the west. Fig. 4b shows that, the peak Θ across line A and peak Sahel rainfall in August are associated with relative low Θ across line B and rain near the Gulf. Moisture comes onshore across line B all year round, except in January when it is near zero. Although Θ is relatively weak (second minimum) in August, it still supplies moisture from the Gulf. In September, the ITCZ may pass the Gulf coast on its southward path and the convection causes the second peak of rain. The reason for the delay in drawing moisture from the Gulf by the convection after the second rain peak needs further investigation.

The equation of water balance in the atmospheric column is

$$\frac{\partial W}{\partial t} + \nabla \cdot \boldsymbol{\Theta} = E - P = F \tag{3}$$

where F is the fresh water exchange between the surface and the atmosphere, the difference between evaporation (E) and precipitation (P) at the surface. The first term is the change of storage. Because of the short residence period of water in the atmosphere, it is negligible for periods longer than synoptic scales, and there should be a balance between the divergence of the transport ($\nabla \cdot \boldsymbol{\Theta}$) and the surface flux. The integral of the divergence of Θ over continental areas should equal the line integral of Θ normal to the boundary (Green's theorem). The total E–P over the Sahel should equal the influx into the area, from the Sahara to the north, and across the mountain in the east, through influx from Gulf of Guinea in the south and from the Atlantic in the west. The water balance of the WAM area, based on moisture transport and its divergence, has been well considered (e.g. Cadet & Nnoli, 1987; Fontaine et al., 2003; Hagos & Zhang, 2010; Meynadier et al., 2010). The results of this study just show that the Atlantic input is more important to the phase of the annual cycle of the Sahel rainfall. This Θ data set has been indirectly validated through continental and global ocean mass balances. The mass change is measured by the Gravity Recovery and Climate Experiment (GRACE), a geodesy mission to measure Earth's gravity field (Tapley et al., 2004). Liu et al. (2006) showed that Θ across the entire coastline of South America, with the river discharge removed, agrees with the mass change of the continent both in magnitude

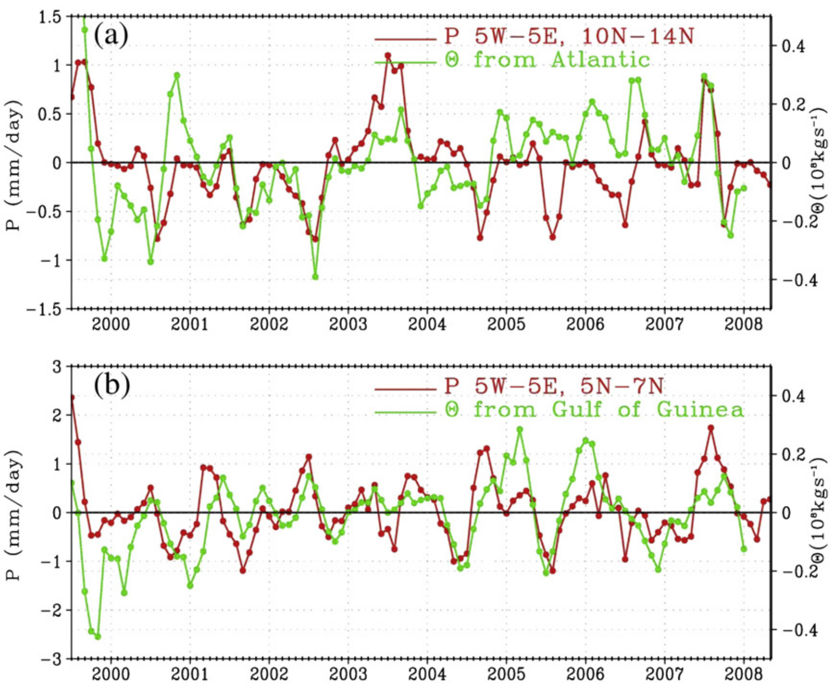

Fig. 9. (a) Time series of the interannual anomalies of TRMM precipitation (red curve) averaged over 5°W–5°E, 10°N–14°N and time series of the integral of Θ component anomalies normal to the coastline A (green curve). (b) Same as (a), except for 5°W–5°E, 5°N–7°N and the coastline B. A 3 month running mean is applied. (For interpretation of the references to color in this figure legend, the reader is referred to the web version of this article.)

and phase of seasonal changes. The surface water flux implied by $\nabla \cdot \mathbf{\Theta}$ was also shown to balance mass change of the global ocean and river discharges in magnitude and phase of the seasonal changes (Liu & Xie, 2008). With the improving spatial resolution of GRACE and the potential capability of the follow-on mission, we may be able to have a more vigorous examination of water balance of the Sahel in the near future.

There is no accurate direct spacebased observation of land evaporation/transpiration, so we could not assess the effect of local factors such as human-induced land cover/use on long-term trends in summer rainfall. New sensors on the Soil Moisture and Ocean Salinity mission (SMOS) (Kerr et al., 2000) and Aquarius (Lagerloef et al., 2008) that measure soil moisture would further our understanding of the local balance between evaporation and rain. The Soil Moisture Active and Passive (SMAP) mission of the National Aeronautic and Space Administration will be launched in a few years. Our ability to measure rainfall over land is expected to be improved by the Global Precipitation Mission (GPM). The results presented here and future satellite data will provide new perspectives and will advance our understanding and prediction of the West African monsoonal rainfall and the processes that control it.

Acknowledgments

This study was conducted at the Jet Propulsion Laboratory (JPL), California Institute of Technology, under contract of the National Aeronautics and Space Administration (NASA). It was jointly supported by the Precipitation Measuring Mission, the Energy and Water Cycle Studies, and Ocean Vector Wind Programs of NASA. Access to the moisture transport data is provided as part of the strategic planning of the JPL Climate Science Center. K.B. Katsaros acknowledges support from the National Science Foundation under grant ATM 0631685.

References

Bell, M. A., & Lamb, P. J. (2006). Integration of weather system variability to multidecadal regional climate change: The West African Sudan-Sahel zone, 1951–98. *Journal of Climate*, *19*, 5343–5365.

Cadet, D. L., & Nnoli, N. O. (1987). Water vapour transport over Africa and the Atlantic Ocean during summer (1979). *Quarterly Journal of the Royal Meteorological Society*, *113*, 581–602.

Chang, P., Zhang, R., Hazeleger, W., Wen, C., Wan, X., Ji, L., et al. (2008). Oceanic link between abrupt changes in the North Atlantic Ocean and the African monsoon. *Nature Geoscience*, *1*, 444–448.

Davey, M., Huddleston, M., Sperber, K. R., Braconnot, P., Bryan, F., Chen, D., et al. (2002). STOIC: A study of coupled model climatology and variability in tropical ocean regions. *Climate Dynamics*, *18*, 403–420.

Fink, A. H., & Reiner, A. (2003). Spatiotemporal variability of the relation between African Easterly waves and west squall lines in 1998 and 1999. *Journal of Geophysical Research*, *108*(D11), 4332, http://dx.doi.org/10.1029/2002JD002816.

Folland, C. K., Palmer, T. N., & Parker, D. E. (1986). Sahel rainfall and worldwide sea temperature 1901–1985. *Nature*, *320*, 602–607.

Fontaine, B., Janicot, S., & Moron, V. (1995). Rainfall anomaly patterns and wind field signals over West Africa in August (1958–1989). *Journal of Climate*, *8*, 1503–1510.

Fontaine, B., Roucou, P., & Trzaska, S. (2003). Atmospheric water cycle and moisture *fluxes* in West African monsoon: mean annual cycles and relationship using NCEP/NCAR reanalysis. *Geophysical Research Letters*, *30*, 1117, http://dx.doi.org/10:1029/2002GL015834.

Giannini, A., Saravanan, R., & Chang, P. (2003). Oceanic forcing of Sahel rainfall on interannual to interdecadal time scales. *Science*, *302*, 1027–1030.

Grodsky, S. A., Carton, J. A., & Nigam, S. (2003). Near surface westerly wind jet in the Atlantic ITCZ. *Geophysical Research Letters*, *30*, 2009, http://dx.doi.org/10.1029/2003GL017867.

Gu, G., & Adler, R. F. (2004). Seasonal evolution and variability associated with the West African monsoon system. *Journal of Climate*, *17*, 3364–3377.

Hagos, S. M., & Cook, K. H. (2007). Dynamics of the West African monsoon jump. *Journal of Climate*, *20*, 5264–5284.

Hagos, S. M., & Zhang, C. (2010). Diabatic heating divergent circulation and moisture transport in the African monsoon system. *Quarterly Journal of the Royal Meteorological Society*, *136*, 411–425.

Hayden, C. M., Menzel, W., Nieman, W. S., Schmit, T., & Velden, C. (1994). Recent progress in methods for deriving winds from satellite data at NESDIS/CIMSS. *Advances in Space Research*, *14*, 99–110.

Hilburn, K. A. (2010). Intercomparison of water vapor transport datasets, Abstract H31H-1098 presented at the 2010 Fall Meeting, AGU, San Francisco, Calif., 13–17 Dec. , http://www.remss.com/papers/hilburn/Hilburn_Transport_Poster_AMS_SatMet_2010_Annapolis.pdf.

Huffman, G. J., Adler, R. F., Bolvin, D. T., Gu, G., Nelkin, E. J., Bowman, K. P., et al. (2007). The TRMM multi-satellite precipitation analysis: Quasi-global, multi-year, combined-sensor precipitation estimates at fine scale. *Journal of Hydrometeorology*, *8*(1), 38–55.

Janicot, S., Trzaska, S., & Poccard, I. (2001). Summer Sahel-ENSO teleconnection and decadal time scale SST variations. *Climate Dynamics*, *18*, 303–320.

Kerr, Y. H., Waldteufel, P., Wigneron, J. P., Martinuzzi, J. M., Lazard, B., Goutoule, J. M., et al. (2000). The soil moisture and ocean salinity (SMOS) mission: An overview. In P. Pampaloni, & S. Paloscia (Eds.), *Microwave Radiometry & Remote Sensing of the Earth's Surface and Atmosphere* (pp. 467–475). The Netherlands: VSP International Publisher.

Lagerloef, G., Colomb, F. R., Le Vine, D., Wentz, F., Yueh, S., Ruf, C., et al. (2008). The Aquarius/SAC-D Mission: Designed to meet the salinity remote-sensing challenge. *Oceanography*, *21*, 68–81.

Lamb, P., & Peppler, A. (1992). Further case studies of tropical Atlantic surface atmospheric and oceanic patterns associated with sub-Saharan drought. *Journal of Climate*, *5*, 476–488.

Le Barbe, L., Lebel, T., & Tapsoba, D. (2002). Rainfall variability in West Africa during the years 1050–90. *Journal of Climate*, *15*, 187–202.

Lebel, T., Diedhiou, A., & Laurent, H. (2003). Seasonal cycle and interannual variability of the Sahelian rainfall at hydrological scales. *Journal of Geophysical Research*, *108*(D8), 8389, http://dx.doi.org/10.1019/2001JD001580.

Liu, W. T. (2002). Progress in scatterometer application. *Journal of Oceanography*, *58*, 121–136.

Liu, W. T., & Tang, W. (2005). Estimating moisture transport over ocean using spacebased observations. *Journal of Geophysical Research*, *110*, D10101, http://dx.doi.org/10,1029/2004JD005300.

Liu, W. T., & Xie, X. (2008). *Latent heat flux and ocean–atmosphere water exchanges. Flux News, 5, 19–21, CLIVAR International Project Office, Southampton, United Kingdom.*

Liu, W. T., Xie, X., Tang, W., & Zlotnicki, V. (2006). Spacebased observations of oceanic influence on the annual variation of South American water balance. *Geophysical Research Letters*, *33*, L08710, http://dx.doi.org/10.1029/2006GL025683.

Matthews, A. J. (2004). Intraseasonal variability over tropical Africa during northern summer. *Journal of Climate*, *17*, 2427–2440.

Meynadier, R., Bock, O., Guichard, F., Boone, A., Roucou, P., & Redelsperger, J. -L. (2010). West African Monsoon water cycle: 1. A hybrid water budget dataset. *Journal of Geophysical Research*, *115*, http://dx.doi.org/10.1029/2010JD013917.

Mortimore, M., & Adams, W. M. (1999). *Working the Sahel.* London: Routledge (240 pp.).

Nicholson, S. E., & Grist, J. P. (2003). The seasonal evolution of the atmosphere circulation over West Africa and equatorial Africa. *Journal of Climate*, *16*, 1013–1030.

Okumura, Y., & Xie, S. P. (2004). Interaction of the Atlantic equatorial cold tongue and he African Monsoon. *Journal of Climate*, *17*, 3589–3602.

Panofsky, H. A., & Brier, G. W. (1968). *Some applications of statistics to meteorology*. University Park: Penn Stat Univ. 224 pp.

Pu, B., & Cook, K. H. (2010). Dynamics of the West African westerly jet. *Journal of Climate*, *23*, 6263–6276.

Redelsperger, J. L., Diongue, A., Diedhiou, A., Ceron, J. -P., Diop, M., Gueremy, J. -F., et al. (2002). Multi-scale description of a Sahelian synoptic weather system representative of the West African monsoon. *Quarterly Journal of the Royal Meteorological Society*, *128*, 1229–1257.

Redelsperger, J. -L., Thorncroft, C. D., Diedhiou, A., Lebel, T., Parker, D. J., & Polcher, J. (2006). African monsoon multidisciplinary analysis. *Bulletin of the American Meteorological Society*, *87*, 1739–1746.

Rienecker, M. M., & coauthors (2011). MERRA: NASA's modern-era retrospective analysis for research and applications. Journal of Climate, 24, 3624–3648.

Rowell, D. P. (2001). Teleconnections between the topical Pacific and the Sahel. *Quarterly Journal of the Royal Meteorological Society*, *127*, 1683–1760.

Rowell, D. P., & Milford, J. R. (1993). On the generation of African squall lines. *Journal of Climate*, *6*, 1181–1193.

Sultan, B., & Janicot, S. (2000). Abrupt shift of the ITCZ over West Africa and intra-seasonal variability. *Geophysical Research Letters*, *27*, 3353–3356.

Sultan, B., & Janicot, S. (2003). The West African monsoon dynamics. Part II: The "preonset" and the summer monsoon. *Journal of Climate*, *16*, 3407–3427.

Tapley, B. D., Bettadpur, S., Ries, J. C., Thompson, P. F., & Watkins, M. (2004). GRACE measurements of mass variability in the Earth system. *Science*, *305*, 503–505.

Vizy, E. K., & Cook, K. H. (2002). Development and application of a mesoscale climate model for the tropics: Influence of sea surface temperature anomalies on the West African monsoon. *Journal of Geophysical Research*, *107*, D34023, http://dx.doi.org/10.1029/2001IJD000686.

WCRP (2011). *Implementing US CLIVAR 2011–2015*. Washington, D.C.: US CLIVAR Office (75 pp.).

Wentz, F. J. (1997). A well-calibrated ocean algorithm for special sensor microwave/imager. *Journal of Geophysical Research*, *102*, 5703–5718.

Xie, X., Liu, W. T., & Tang, B. (2008). Spacebased estimation of moisture transport in marine atmosphere using support vector regression. *Remote Sensing of Environment*, *112*, 1845–1855.

Zheng, X., Eltahir, A. B., & Emanuel, K. A. (1999). A mechanism relating tropical Atlantic spring sea surface temperature and West African rainfall. *Quarterly Journal of the Royal Meteorological Society*, *125*, 1129–11163.